Structure of Polyelectrolytes in Solution: A Monte Carlo Study

Heiko Schäfer† and Christian Seidel*

Max-Planck-Institut für Kolloid- und Grenzflächenforschung, Kantstrasse 55, D-14513 Teltow-Seehof, Germany

Received December 27, 1996; Revised Manuscript Received July 14, 1997⊗

ABSTRACT: Monte Carlo simulations have been used to study strongly charged chains in solution. The charges on the chains are assumed to interact with a screened Coulomb potential of the Debye−Hückel type. Similarly to the behavior obtained in simulations with the full long range interaction, the single-chain structure factor exhibits different scaling regimes at short and large length scales, respectively. To examine the effect of interchain interaction, we compare the many-chain results with single-chain simulations done at the same degree of screening. In agreement with other simulations but in contradiction to theory, at finite polymer concentration the chains are found to contract well below the overlap density.

I. Introduction

Despite the enormous interest in polyelectrolytes, the present understanding of their behavior is rather poor, in contrast to the knowledge on uncharged polymers (see, e.g., refs 1 and 2). The lack of understanding results from specific difficulties in experimental, theoretical, and simulation studies. The theoretical description of flexible polyelectrolytes is handicapped by the fact that up to now the full Coulomb potential is intractable for flexible chains. Therefore, most of the theoretical studies as well as simulations have been done within a jellium type model where all low molecular weight ions (counterions as well as additional salt ions) are assumed to be homogeneously smeared throughout the solution. The resulting screened interaction can be described by a Debye−Hückel (DH) potential. Besides that, most theoretical works start from a rigid rod or at least from a locally rigid chain to model polyelectrolytes. Obviously, the role of entropy is neglected or underestimated in such models. Not to mention that there are different theoretical predictions on the relation between persistence length L_p and screening length λ_D,[3−5] the general picture suggested by theory is as follows: (i) The chains can be considered as a sequence of rods each of length L_p; i.e., on short length scales the chain should be stiff with a Flory exponent $\nu = 1$.[3,6,7] (ii) At large scales $s \gg L_p$, the expectation is that the influence of the short range DH potential is reduced to an electrostatic contribution to the excluded volume $v_e \sim 8\pi L_p{}^2\lambda_D$; i.e., the behavior should be similar to that of neutral chains in a good solvent.[8] Although simulations that treat individual counterions[9,10] have shown that fluctuations in the counterion density have a significant effect on the mean structure of linear polyelectrolytes, it is still of interest to study Debye−Hückel chains by simulations in order to check the theoretical predictions mentioned above which have been obtained within the Debye−Hückel approximation.[11−13]

The outline of the paper is as follows. We first give a short summary of the model and the simulation method used in the study. In the next section we discuss the results on the single-chain structure factor in many-chain systems and compare them to single-chain simulations at the same degree of screening. In the last section we conclude with a comparison of the results obtained in simulations that treat individual counterions and the full long range interaction.

II. Model and Simulation Method

In order to study the behavior of flexible polyelectrolyte chains in solution by standard Metropolis Monte Carlo simulation, we use the bond fluctuation algorithm introduced by Carmesin and Kremer.[14] This is a fast lattice algorithm that in three dimensions offers a set of 108 bond vectors with five different lengths. In contrast to usual lattice algorithms, one monomer does not occupy one lattice site but eight sites in three dimensions. Enforcing excluded volume by prohibiting multioccupied lattice sites, we take the chains to be in a good solvent.

In order to have a force that counteracts the repulsive electrostatic interaction between charged monomers, we introduce a harmonic bond potential:

$$U_{\text{bond}}(l) = \frac{k}{2}(l - \bar{a})^2 \tag{1}$$

where l is the length of the corresponding bond vector. The average bond length of neutral chains without bond potential was checked to be $\bar{a} = 2.694a_0$ with a_0 being the spacing of the underlying lattice. The spring constant k can be determined by taking the second derivative of the Lennard-Jones (LJ) potential and assuming that the minimum of the potential occurs at a distance equal to the average bond length: $\bar{a} = 2^{1/6}\sigma$. This condition yields $k = 72\epsilon/\bar{a}^2$.

Each of the M chains in the simulation box of volume L^3 consists of N monovalent monomers. Thus we have a total number of $N_{\text{tot}} = M \times N$ charged monomers. Electroneutrality requires the existence of a corresponding counter charge, which we assume to consist of N_{tot} monovalent counterions. Besides that, salt can be added to increase the screening of the interaction. Within the present model, salt and counterions are not treated explicitly. We rather assume that they form a homogeneous background by treating the electrostatic interactions using the Debye−Hückel approximation, which yields the effective potential

$$\frac{U_{\text{DH}}(r)}{k_B T} = \frac{\lambda_B}{r}\exp\left[-\frac{r}{\lambda_D}\right] \tag{2}$$

where $\lambda_B = e^2/4\pi\epsilon\epsilon_0 k_B T$ is the Bjerrum length. The strength of the interaction is given by the dimensionless coupling constant (Manning parameter) $\Gamma = \lambda_B/\bar{a}$, while its range depends on the screening length (Debye

* To whom correspondence should be addressed.

† Present address: Laboratorium für Physikalische Chemie, ETH Zentrum, CH-8092 Zürich, Switzerland.

⊗ Abstract published in *Advance ACS Abstracts,* October 1, 1997.

S0024-9297(96)01906-7 CCC: $14.00

Table 1. Simulated Systems

N	M	N_{tot}	ϕ
16	20	320	$0.1-10^{-3}$
16	40	640	2×10^{-4}
32	8	256	$0.1-1.2 \times 10^{-3}$
32	20	640	2×10^{-4}
64	10	640	$0.2-2 \times 10^{-4}$
80	8	640	$0.1-2 \times 10^{-4}$

length) $\lambda_D = (1/4\pi\lambda_B n)^{1/2}$ with n = $c_{ci} + 2c_s$ being the number density of monovalent ions where $c_{ci} = c = N_{tot}/L^3$ is the corresponding density of counterions and c_s that of salt. Thus, in the salt-free case, box length and Debye length are related by $L = (4\pi N_{tot}\lambda_B\lambda_D^2)^{1/3}$. The exponential in eq 2 enables the introduction of a cutoff, which we define as a multiple of the Debye length $\lambda_c = m\lambda_D$. On the other hand, due to the minimum image condition, one has to guarantee $\lambda_c < L/2$. The latter condition gives an upper limit of the screening length with $\lambda_D < (\pi/2)\lambda_B N_{tot}/m^3$. Most of the simulations have been done with a cutoff of $m = 5$. However, in order to extend the accessible density range at a restricted number of particles $N_{tot} = 640$, for the lowest densities the cutoff was reduced to $m = 4$. According to Manning,[15] counterion condensation is expected to occur if the distance between charges becomes smaller than the Bjerrum length. To avoid these problems, we set the spacing of the underlying lattice by the relation $\bar{a} = 1.1\lambda_B = 2.694a_0$. The Bjerrum length in water at room temperature is 7.14 Å. Hence, the polyelectrolyte chains are modeled on a coarse-grained level where the charge separation is 7.85 Å. The bond length for, e.g., NaPSS is about 2.5 Å. Thus, depending on the roughness of the chains the fraction of charged monomers is $f = 0.14-0.33$. As a measure for the monomer density we use the volume fraction of occupied lattice sites $\phi = 8N_{tot}/(L/a_0)^3$. The density in LJ units is given by $\rho\sigma^3 = \sigma^3 N_{tot}/L^3 = \phi(\sigma/2a_0)^3$. Using the mean bond length to map roughly ϕ on ρ, one obtains the relation $\rho\sigma^3 \approx 1.728\phi$. For NaPSS, our volume fraction of $\phi = 0.001$ corresponds to a monomer concentration of about 1.4×10^{-2} mol/L. The simulated systems and density regions are given in Table 1.

Ensemble-averaged chain properties are taken as averages (i) over typically 0.5×10^6 Monte Carlo steps per monomer, which corresponds to at least 6×10^5 renewal times, and (ii) over the M chains in the box. All the simulations of many-chain systems have been done with two different starting initializations. The single-chain results are based on an average over 9 or 4 independent chains. In this way the results on the m.s. end-to-end distance, the m.s. radius of gyration, and the persistence length were found to be reproducible within a few percent.

III. Results and Discussion

In this paper we discuss the single-chain structure factor $S(\boldsymbol{q})$ as a function of monomer density ranging from the semidilute to dilute regime. This is a convenient way in theory as well as in simulation studies to describe the chain structure at all length scales. Moreover, $S(\boldsymbol{q})$ is a quantity directly accessible to scattering experiments on polymer solutions. We use the spherically averaged structure factor $S(q)$

$$S(q) = \frac{1}{N}\langle\langle|\sum_{n=1}^{N}\exp(i\mathbf{q}\mathbf{r}_n)|^2\rangle_{|\mathbf{q}|}\rangle$$

where $\boldsymbol{r}_n$ is the position of the nth segment. The normalization is $S(0) = N$. Within the region $2\pi/R < q < 2\pi/a$ where R is the averaged end-to-end distance, $S(q)$ scales as $S(q) \propto q^{-1/\nu}$. Hence, one has a direct way to estimate the Flory exponent ν. From Figure 1, where $S(q)$ is shown for four different chain lengths at $\phi = 2 \times 10^{-4}$, one can conclude that the chain structure is chain length independent over the range $q > 2\pi/R$. Hence, on length scales up to $R(N = 80)$ we can extrapolate the results even to chains longer than $N = 80$. Figure 2 shows the density dependence of the single-chain structure factor for $N = 64$. It indicates drastic changes in the coil structure below the overlap density ϕ^*, which lies between $\phi = 0.01$ and $\phi = 0.1$ in our systems. Since in the semidilute regime the Debye length becomes smaller than the bond length we obtain almost no effect due to electrostatic interaction. However, this can be considered as an artifact of the DH approximation, which is known to break down in the high-density regime.[16] Apart from the vanishing effect of electrostatic repulsion, in the high-density limit we obtain nearly ideal behavior with $\nu \approx 1/2$ due to strong Edwards screening of the excluded volume.

The most interesting feature, however, is the existence of two distinct scaling regimes at densities below ϕ^*. This is shown in detail for the $N = 64$ chains at $\phi = 2 \times 10^{-4}$ in Figure 3. Below the bond peak, the Porod region starts with regime 1, which reflects the behavior at short length scales. After passing a crossover region,

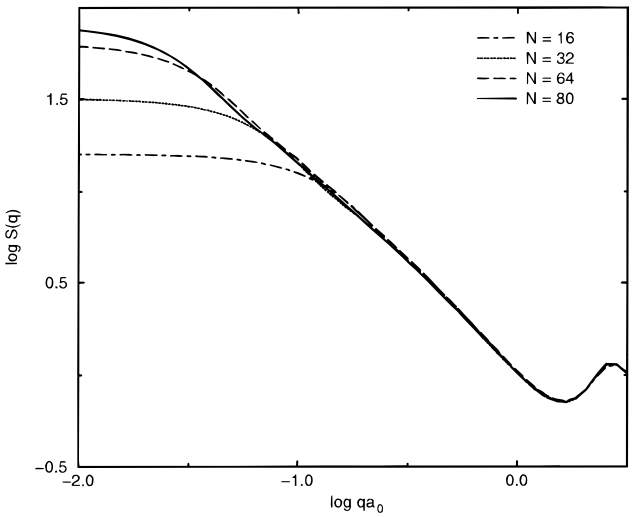

Figure 1. Single-chain structure factor for $N = 16$, 32, 64, and 80 at $\phi = 2 \times 10^{-4}$.

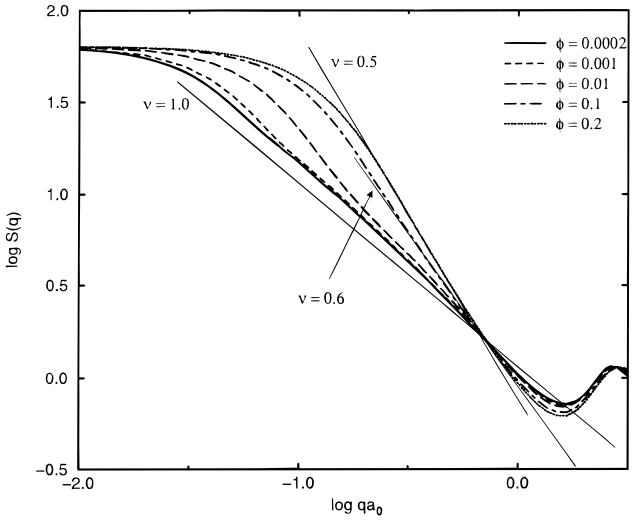

Figure 2. Single-chain structure factor as a function of density for $N = 64$.

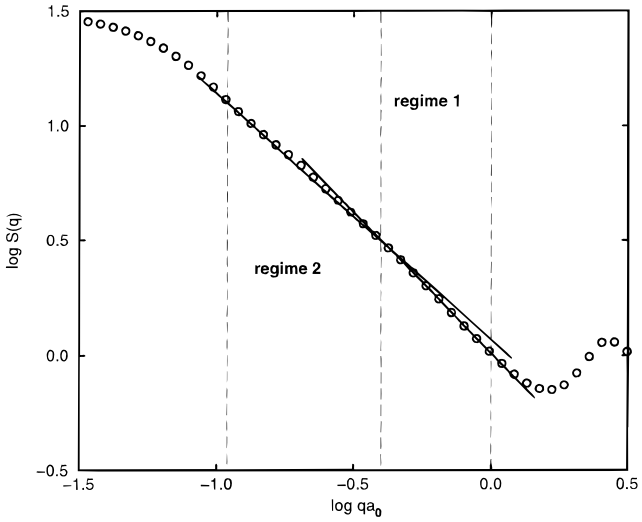

Figure 3. Different scaling regimes in the single-chain structure factor for $N = 64$, $\phi = 2 \times 10^{-4}$. Regime 1 corresponds to the behavior at short length scales, while regime 2 reflects large scale behavior.

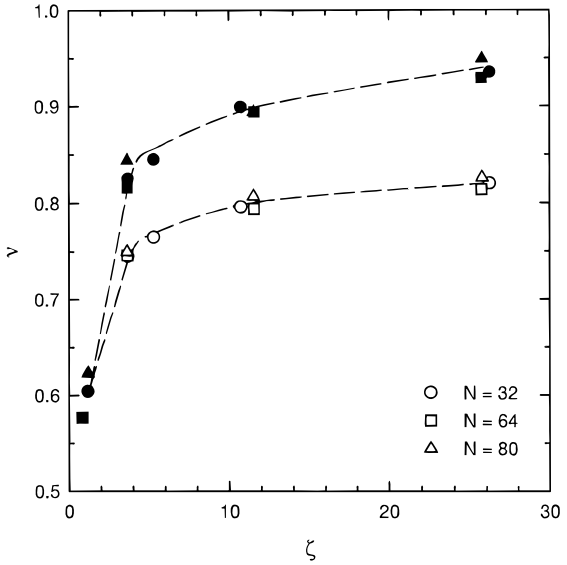

Figure 4. Density dependence of the scaling exponents shown as a function of the screening parameter $\zeta = 2\lambda_D/\bar{a}$. Open symbols correspond to the short scale behavior (regime 1); solid symbols, to the large scale one (regime 2). The dashed lines are a guide for the eyes.

the slope becomes less negative and we enter a second scaling regime that corresponds to large length scales. The crossover region shows no clear dependency on density or chain length, but converted into length scales it appears in all cases at about $6\bar{a}$. Figure 4 shows the ν exponents following from the structure factor. They are plotted against the screening parameter $\zeta = 2\lambda_D/\bar{a}$. Within our model and using the parameters as set above, ζ is related to the density by $\zeta \approx 0.5(\rho\sigma^3)^{-1/2}$. Both exponents vary continuously with the strength of screening but the exponent corresponding to short length scales ν_{sl} (regime 1) is always smaller than the large scale exponent ν_{ll} (regime 2). Starting at $\phi = 0.1$ ($\zeta \approx 1.2$), we are in the semidilute regime where the chains basically behave like neutral polymers in a good solvent; i.e., there is only one scaling regime at all length scales with $\nu \approx 0.6$. However, entering the dilute regime immediately there occur two different regimes. The short scale exponent, ν_{sl}, seems to have a limiting value near $\nu_{sl} \approx 0.85$, i.e., far below $\nu = 1$. For the short length scale behavior, saturation at large screening lengths is quite reasonable because λ_D becomes much larger than the crossover length. However, a saturation value smaller than 1 is in contradiction with almost all theories,[3−5] as they predict locally stiff chains on scales of the persistence length. On the other hand, the behavior is in agreement, at least qualitatively, with results of MD simulations that explicitly treat the counterions.[9,10] Stevens and Kremer found that the short length scale regime occurs at a characteristic length scale, which they estimated to be in the range of six average bond lengths. Apart from a rescaling of the number of monomers that might be necessary to compare the different models,[17] this characteristic length is in good agreement with our data. Hence, the chains are predicted to remain rough on small length scales. This seems to be a result of the competition between the loss of entropy by taking a stretched conformation versus the gain in energy by having maximum distance between neighboring charges. The crucial point is the constraint imposed by the connectivity of the chain, which prevents the chain from gaining a large amount of energy on small length scales. Including fluctuation corrections, Li and Witten[18] studied the balance between the two competing factors in detail. These calculations show that for distances smaller than the screening length, the fluctuations in the chain conformation get stronger due to softening of small-wavelength modes, giving rise to the roughness on small length scales. In contrast to the behavior obtained by Stevens and Kremer,[9,10] we do not find, however, the density independence of ν_{sl}. Presumably, this universal behavior is related to the presence of individual counterions and cannot be reproduced by a homogeneous background within the Debye−Hückel approximation. On large length scales the chains are more stretched than on short ones. Unfortunately, for most of our systems, we did not yet reach vanishing intrachain screening at $\lambda_D \gg R$. Therefore, on the basis of the data available so far, we cannot decide whether complete stretching with $\nu_{ll} = 1$ appears in the low-density limit or not. However, obviously there is a tendency that the shorter the chains the closer to saturation they are at the lowest density ($\phi = 2 \times 10^{-4}$), i.e., at the largest screening parameter ζ shown in Figure 4.

In order to examine the effect neighboring chains have on the configuration of an individual chain, we compare some results on $S(q)$ discussed above for many-chain systems ($N = 64$, $M = 10$) with single-chain simulations done at the same degree of screening (which can be realized by adding salt). The corresponding single-chain structure factors are shown in Figures 5 and 6. At strong screening $\lambda_D < \bar{a}$ (case a in Figure 5, i.e., $\phi = 0.2$, $\lambda_D = 1.1a_0$), a fundamental difference appears between the two systems. While in the many-chain system the individual chains are strongly coiled with a Flory exponent of $\nu = {}^1/_2$, we obtain good solvent behavior with $\nu \approx 0.6$ in the corresponding single-chain system. This is, however, a pure polymer screening effect, which has no relation to electrostatic interaction. Because the density of the corresponding many-chain system is above ϕ^*, excluded volume is suppressed by Edwards screening while the single-chain exhibits the behavior of a neutral chain in a good solvent. Near but below the transition from semidilute to dilute regime (case b in Figure 5, i.e., $\phi = 10^{-2}$, $\lambda_D = 5.0a_0$), differences between single and many-chain systems occur only at large length scales of the order of R. In this concentration range, due to $\lambda_D \approx 2\bar{a}$, the interaction is sufficiently short ranged and the chains are still well coiled. Therefore, first of all, the more mobile chain ends are

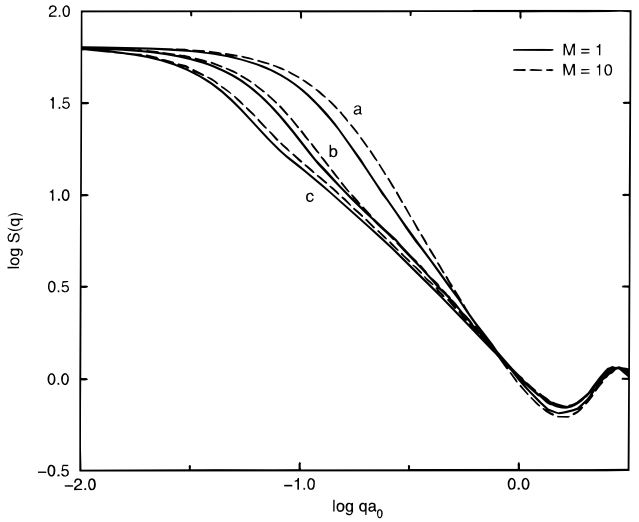

Figure 5. Single-chain structure factor of many-chain systems ($M = 10$) in comparison with that of corresponding single-chain systems ($M = 1$) as a function of screening (density) at (a) $\lambda_D = 1.1a_0$ ($\phi = 0.2$), (b) $\lambda_D = 5.0a_0$ ($\phi = 10^{-2}$), and (c) $\lambda_D = 16.2a_0$ ($\phi = 10^{-3}$).

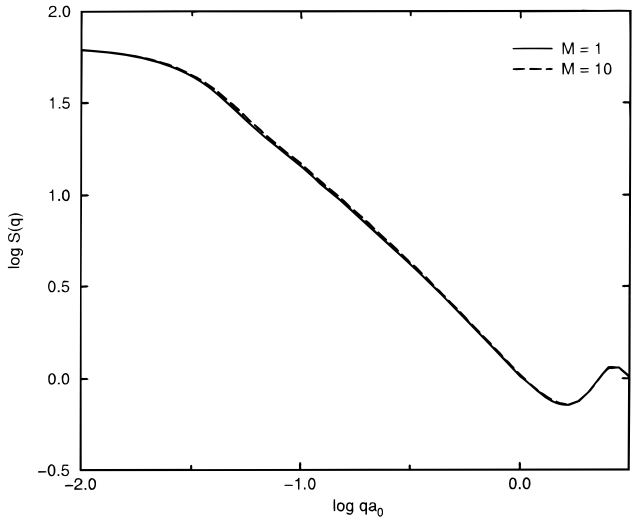

Figure 6. As Figure 5 but at $\lambda_D = 36.1a_0$ ($\phi = 2 \times 10^{-4}$).

expected to experience neighboring coils. In case c shown in Figure 5 ($\phi = 10^{-3}$, $\lambda_D = 16.2a_0$), we are well below ϕ^*. Now the chains are rather elongated with a Flory exponent $\nu_{ll} \approx 0.9$. However, as a result of the interchain repulsion the chains appear to undergo a coiling over almost all length scales. In this way the chains reduce their overlap at the expense of intrachain energy. On the other hand, compared to a highly elongated shape, there is also an additional gain in entropy that favors coiling. Finally, from Figure 6 one can see that at the lowest density the structure of the individual chains is almost not influenced by their neighbors.

IV. Conclusion

We have performed Monte Carlo simulations of polyelectrolytes in salt-free solution and of single polyelectrolyte chains in solution with added salt. The Coulomb interaction is treated within the Debye−Hückel approximation. Information on the structure of the chains is deduced from the single-chain structure factor. Similarly to the behavior obtained in simulations that explicitly treat the counterions,[9,10] two distinct scaling regimes appear at densities below ϕ^*. Instead of becoming very stretched on all lengths scales, as proposed by theory, the chains remain rough on short length scales but avoid bends on large length scales. Both the corresponding exponents ν_{sl} and ν_{ll} vary continuously as a function of density (or as a function of salt concentration in the single-chain system). The short scale exponent ν_{sl} shows saturation at low densities with a limiting value near $\nu_{sl} \approx 0.85$. This value confirms the short scale structure proposed by Stevens and Kremer. However, we did not observe the density independence. Probably this is due to the DH approximation and the related lack of individual counterions. Concerning the large length scales behavior the situation is not completely clear yet. On the basis of the data available so far, we cannot decide whether for DH chains $\nu_{ll} = 1$ can be reached or not.

To examine the effect neighboring chains have on the configuration of an individual chain, we compare the behavior of many-chain systems with that of the corresponding single-chain ones where the screening length has been adjusted by adding salt. At the lowest density, the elongated structure of the individual chains is almost not influenced by the presence of neighboring chains. However, already far below the overlap density we observe a contraction of the chains in the many-chain system. The chains begin to coil in order to stay as isolated objects rather than to maintain a highly elongated shape and to overlap. This behavior is in contradiction with theoretical predictions[3,6,7,19] but in agreement, at least qualitatively, with the results earlier obtained by Stevens and Kremer[9,10] in MD simulations with explicit counterions. At higher densities but still below ϕ^* differences in the chain structure appear only at large length scales in the order of the end-to-end distance R. This is probably an effect of both the coiled structure of the chains and the small screening length.

Completing the paper, we learned about a MD simulation of DH chains done by Stevens and Kremer,[20] who obtained features of the single-chain structure factor at finite polymer concentration that are similar to some of our results found by MC simulation in a different model.

References and Notes

(1) Dautzenberg, H.; et al. *Polyelectrolytes: Formation, Characterization and Application*; Hanser Publishers: Munich, Vienna, New York, 1994.
(2) Förster, S.; Schmidt, M. *Adv. Polym. Sci.* **1995**, *120*, 53.
(3) de Gennes, P. G.; Pincus, P.; Velasco, R. M.; Brochard, F. *J. Phys. Fr.* **1976**, *37*, 1461.
(4) Odijk, T. *J. Polym. Sci., Polym. Phys. Ed.* **1977**, *15*, 477.
(5) Scolnick, J.; Fixman, M. *Macromolecules* **1977**, *10*, 944.
(6) Hayter, J.; Jannink, G.; Brochard-Wyart, F.; de Gennes, P. G. *J. Phys. Fr. Lett.* **1980**, *41*, L451.
(7) Odijk, T. *Macromolecules* **1979**, *12*, 688.
(8) Odijk, T.; Houwaart, A. C. *J. Polym. Sci., Polym. Phys. Ed.* **1978**, *16*, 627.
(9) Stevens, M. J.; Kremer, K. *Macromolecules* **1993**, *26*, 4717.
(10) Stevens, M. J.; Kremer, K. *J. Chem. Phys.* **1995**, *103*, 1669.
(11) Ullner, M.; Jönsson, B.; Söderberg, B.; Peterson, C. *J. Chem. Phys.* **1996**, *104*, 3048.
(12) Seidel, C. *Ber. Bunsen-Ges. Phys. Chem.* **1996**, *100*, 757.
(13) Micka, U.; Kremer, K. *Phys. Rev. E* **1996**, *54*, 2653.
(14) Carmesin, I.; Kremer, K. *Macromolecules* **1988**, *21*, 2819.
(15) Manning, G. S. *J. Chem. Phys.* **1969**, *51*, 924.
(16) Dobrynin, A. V.; Colby, R. H.; Rubinstein, M. *Macromolecules* **1995**, *28*, 1895.
(17) Gerroff, I.; Milchev, A.; Binder, K.; Paul, W. *J. Chem. Phys.* **1993**, *98*, 6526.
(18) Li, H.; Witten, T. A. *Macromolecules* **1995**, *28*, 5921.
(19) Witten, T.; Pincus, P. *Europhys. Lett.* **1987**, *3*, 315.
(20) Stevens, M. J.; Kremer, K. *J. Phys. II Fr.* **1996**, *6*, 1607.

MA961906L